



Published in final edited form as:

*Mol Cancer Res.* 2020 April ; 18(4): 623–631. doi:10.1158/1541-7786.MCR-19-0741.

## Combined Src/EGFR inhibition targets STAT3 signaling and induces stromal remodeling to improve survival in pancreatic cancer

Austin R. Dosch<sup>1,2</sup>, Xizi Dai<sup>1,2</sup>, Michelle L. Reyzer<sup>3</sup>, Siddharth Mehra<sup>1,2</sup>, Supriya Srinivasan<sup>1,2</sup>, Brent A. Willobee<sup>1,2</sup>, Deukwoo Kwon<sup>4</sup>, Nilesh Kashikar<sup>5</sup>, Richard Caprioli<sup>3</sup>, Nipun B. Merchant<sup>1,2,\*</sup>, Nagaraj S. Nagathihalli<sup>1,2,\*</sup>

<sup>1</sup>Division of Surgical Oncology, Department of Surgery, University of Miami Miller School of Medicine, Miami, Florida;

<sup>2</sup>Sylvester Comprehensive Cancer Center, University of Miami, Miami, Florida;

<sup>3</sup>Mass Spectrometry Research Center, Vanderbilt University, Nashville, Tennessee;

<sup>4</sup>Department of Public Health, University of Miami Miller School of Medicine, Miami, Florida;

<sup>5</sup>Department of Pathology, University of Colorado, Denver, Colorado.

### Abstract

Lack of durable response to cytotoxic chemotherapy is a major contributor to the dismal outcomes seen in pancreatic ductal adenocarcinoma (PDAC). Extensive tumor desmoplasia and poor vascular supply are two predominant characteristics which hinder the delivery of chemotherapeutic drugs into PDAC tumors and mediate resistance to therapy. Previously, we have shown that STAT3 is a key biomarker of therapeutic resistance to gemcitabine treatment in PDAC which can be overcome by combined inhibition of the Src and EGFR pathways. Although it is well-established that concurrent EGFR and Src inhibition exert these anti-neoplastic properties through direct inhibition of mitogenic pathways in tumor cells, the influence of this combined therapy on stromal constituents in PDAC tumors remains unknown. In the present study, we demonstrate in both orthotopic tumor xenograft and *Ptf1a<sup>cre/+</sup>;LSL-Kras<sup>G12D/+</sup>;Tgfb<sup>2</sup><sup>flx/flx</sup>* (PKT) mouse models that concurrent EGFR and Src inhibition abrogates STAT3 activation, increases microvessel density (MVD), and prevents tissue fibrosis *in vivo*. Furthermore, the stromal changes induced by parallel EGFR and Src pathway inhibition resulted in improved overall survival in PKT mice when combined with gemcitabine. As a Phase 1 clinical trial utilizing concurrent EGFR and Src inhibition with gemcitabine has recently concluded, these data provide timely translational insight into the novel mechanism of action of this regimen and expand our understanding into the phenomenon of stromal-mediated therapeutic resistance.

**Corresponding Authors:** Nagaraj S. Nagathihalli and Nipun B. Merchant, Division of Surgical Oncology, Department of Surgery, University of Miami Miller School of Medicine, 1550 NW 10th Ave, FOX140L, Miami, Florida 33136. Phone: 305-243-3502. [nnagathihalli@med.miami.edu](mailto:nnagathihalli@med.miami.edu); [nmerchant@miami.edu](mailto:nmerchant@miami.edu).

\*Indicates co-senior/corresponding authors

**Conflict of Interest:** The authors declare no potential conflicts of interest.

## Keywords

Pancreatic cancer; Src kinase; EGFR; chemoresistance; stroma

---

## Introduction

Pancreatic ductal adenocarcinoma (PDAC) carries a dismal prognosis which is scarcely improved by administration of cytotoxic chemotherapy (1). Recent efforts have utilized molecularly targeted therapies to inhibit constitutively activated kinase pathways in PDAC and improve tumor response to chemotherapy. Small molecule inhibitors of the epidermal growth factor receptor (EGFR) and the non-receptor tyrosine kinase Src initially emerged as promising therapeutic targets due to their effects on multiple downstream mediators which are activated in PDAC (2). However, single-agent EGFR or Src inhibition in combination with conventional chemotherapy has proven ineffective in human clinical trials, namely due to the persistence of cellular feedback mechanisms which foster therapeutic resistance to single agent kinase inhibitors (3–5). Reactivation of the signal transducer and activator of transcription 3 (STAT3) pathway has been shown to be a key mediator of resistance to monotherapy with either EGFR or Src inhibitors (6,7). We have previously demonstrated that simultaneous inhibition of Src kinase and EGFR signaling blocks activation of the oncogenic transcription factor STAT3 to overcome therapeutic resistance and improve the efficacy of gemcitabine (GEM) through inhibiting proliferation, invasion, and inducing apoptosis in PDAC tumor cells *in vitro* (8). However, the efficacy of this regimen on reducing stromal fibrosis and improving overall survival in PDAC *in vivo* remain unknown.

The fibrotic, hypovascular PDAC tumor microenvironment (TME) is unique among solid organ cancers and contributes heavily to the development of therapeutic resistance by limiting vascular perfusion, fostering tissue hypoxia, and acting as a mechanical barrier to drug delivery (9,10). Preceding efforts have explored strategies to both curtail and reverse fibrosis in PDAC in order to enhance the infiltration of cytotoxic compounds into tumors (11). However, conflicting experimental evidence and lack of clinical efficacy has highlighted the need for alternative strategies to target the stroma in PDAC (12,13). We have previously shown that direct pharmacologic inhibition of STAT3 combats stromal-mediated chemoresistance by suppressing fibrosis and increasing microvessel density (MVD) in the TME, thereby augmenting the infiltration of GEM into PDAC tumors to improve overall survival in a murine model of PDAC (14). As our former studies have shown combined Src/EGFR blockade potently inhibits STAT3 activation in PDAC tumors, we hypothesized that concurrent Src/EGFR inhibition would affect the tumor stroma similarly to STAT3 monotherapy (8). In this investigation, we confirm that dual therapy with the Src inhibitor, dasatinib (DST), and the EGFR kinase inhibitor, erlotinib (ERL), inhibits STAT3 activity, induces stromal remodeling, and enhances MVD in PDAC tumors, resulting in an improvement in overall survival in *Ptf1a<sup>cre/+</sup>;LSL-Kras<sup>G12D/+</sup>;Tgfbr2<sup>flox/flox</sup>* (PKT) transgenic mice. As investigations into the use of combined Src/EGFR inhibition for the treatment of PDAC are currently in early stage clinical trials, these data provide timely insight into the novel mechanism of action of these compounds and expand our understanding into the phenomenon of stromal-mediated therapeutic resistance.

## Materials and Methods

### Animals

Athymic nude mice, Fox1 *nu/nu* (4–6 weeks old), were purchased from Harlan Sprague Dawley, Inc. (Indianapolis, IN). The genetically engineered *Ptf1a<sup>cre/+</sup>;LSL-Kras<sup>G12D/+</sup>;Tgfbr2<sup>fllox/fllox</sup>* (PKT) mouse models (provided by Dr. Harold Moses, Vanderbilt University Medical Center, Nashville, TN) were bred as previously described (14,15).

### Cell Lines and orthotopic tumor models

Human pancreatic cancer cell lines BxPC3 and PANC1 were obtained from American Type Culture Collection (ATCC) and maintained according to the ATCC guidelines. Cell authentication was performed by using STR DNA profiling (latest date: June 16, 2016) and cell lines tested negative for Mycoplasma via Genetica cell line testing (Burlington, NC, USA) using eMYCO plus kit (iNtRON Biotechnology). Cells with low passage numbers (< 20) were used. ATCC cell lines were characterized and were free of Mycoplasma contamination, tested by Hoechst DNA stain (indirect) and agar culture (direct) methods. Orthotopic cell injections, intraoperative monitoring, and post-operative analgesia were performed as previously described (14). Briefly, orthotopic tumors were established by injection of  $2.5 \times 10^6$  BxPC3 and PANC1 cells into the pancreata of female athymic nude mice. Mice were treated as single-arm or in combination with the Src kinase inhibitor, dasatinib (DST, 25 mg/kg, oral gavage twice daily), the EGFR tyrosine kinase inhibitor, erlotinib (ERL, 50 mg/kg, oral gavage daily), and/or gemcitabine (GEM, 15 mg/kg, intraperitoneal injection three times weekly) and compared to vehicle (citrate buffer) treated mice (n=5 mice in each treatment arm for each cell line xenograft). For endpoint analysis, treatment was maintained for three weeks, after which mice were sacrificed and tumors extracted for histologic analysis.

### Treatment of *Ptf1a<sup>cre/+</sup>;LSL-Kras<sup>G12D/+</sup>;Tgfbr2<sup>fllox/fllox</sup>* (PKT) mice

Treatment of vehicle, DST (25 mg/kg, oral gavage twice daily), ERL (50 mg/kg, oral gavage daily), and/or GEM (15 mg/kg, intraperitoneal injection three times weekly) in PKT mice was initiated at four weeks of age, at the point where mice develop locally invasive, rapidly progressive tumors (15). Treatment was implemented for four weeks in endpoint analysis arm, upon which mice were sacrificed. For survival analysis, treatment was continued in PKT mice until they were moribund.

All animal experiments were performed in accordance with Institutional Animal Care and Use Committees at Vanderbilt University (Nashville, TN) and The University of Miami (Miami, FL) (Protocol #15–057, 15–099 and 18–081).

### Immunohistochemistry (IHC)

Pancreatic tumor sections were isolated from both PKT mice and orthotopic xenografts and fixed in 10% neutral buffered formalin solution. Tissue slides were then deparaffinized followed by heat induced antigen retrieval in citrate buffer (pH = 6.0). This was followed by quenching endogenous peroxidase activity by incubating in 3% H<sub>2</sub>O<sub>2</sub> for ten minutes. Tissues were further immunostained using indicated primary antibodies (Supplementary

Table S1). Primary antibodies were then detected using VECTASTAIN Elite ABC peroxidase kit as per the manufacturer's protocol using diaminobenzidine (DAB) as the chromogen. Finally, the sections were counterstained with Mayer's hematoxylin and mounted with D.P.X. Tissue sections and were microscopically examined. Digital slide images were adjusted to exclude areas containing histologic artifacts, such as tissue folds or nonorganic material, from the digital image. Positive staining was quantified by using ImageJ image analysis software (NIH) and reported as percentage area of staining. Trichrome blue staining was performed as previously described (14). PKT tumor tissues from four week endpoint analysis arm were additionally stained using hematoxylin and eosin. Total tumor area relative to normal pancreas was estimated in these sections by manual quantification of random fields.

### Western Blot Analysis

Western blot analysis was performed using standard methods previously described (16). Primary antibodies (listed in Supplementary Table S1) were incubated overnight at 4<sup>0</sup>C. In brief, after treatment, pancreas tissues from PKT mice were homogenized in RIPA buffer with protease inhibitor cocktail (Sigma, St. Louis, MO) and PhosSTOP phosphatase inhibitor (Roche, Indianapolis, IN, USA) for protein preparations. Homogenates of tumor samples were subjected to SDS-PAGE followed by Western blotting. Immunoblots were quantified using ImageJ and analysis was performed with Prism software (Graphpad Software Inc., La Jolla, CA).

### Matrix-assisted laser desorption/ionization imaging mass spectrometry (MALDI-IMS)

MALDI-IMS experiments were performed as previously described (14). In brief, BxPC3 tumor xenografts were removed and flash-frozen in liquid nitrogen before storage at -80°C. Frozen tissue samples were then cut into 12 µm thick sections using a cryostat (Leica Microsystems, Buffalo Grove, IL). These frozen sections were then thaw-mounted onto gold-coated, stainless steel MALDI target plates. Matrix solution (2',4',6'-trihydroxyacetophenone, 20 mg/mL in 60:40 methanol:water with 0.1% trifluoroacetic acid) was manually applied to tissues using a glass nebulizer. MALDI mass spectra were acquired using a linear ion trap (LTQ XL) mass spectrometer (Thermo Fisher Scientific) in MS/MS mode. MS/MS was performed on the protonated parent ion of gemcitabine (m/z 264) and full product ion spectra were obtained, allowing GEM to be differentiated by pseudo-selected reaction monitoring. The main fragment ion of gemcitabine at m/z 112 was utilized for image reconstruction. Spectra were obtained for each section at 150 µm spatial resolution. Images were generated using ImageQuest software (Thermo Fisher Scientific) by analyzing the main fragment ion intensity as a function of the position over the tissue surface. For statistical comparisons, average spectra were generated over each tissue section and the intensities of m/z 112 were exported for further comparisons.

### Statistical Analysis

Statistics were calculated using Microsoft Excel, Prism software, and statistical software package R (version 3.3.2). Statistical analyses of immunohistochemistry experiments were analyzed using one-way ANOVA to assess the differences between experimental groups after raw image analysis using ImageJ software (NIH). Analysis of MALDI-IMS data were

performed using Student's t-test with  $P < 0.05$  taken as significant, except where otherwise noted. Overall survival was determined using Kaplan-Meier plot and log-rank test in Prism software. P-values were obtained from permutation test to compare adjusted area under the curve (aAUC) of body weight curves between groups as previously described (17). All statistical analysis was reviewed by the Biostatistic and Bioinformatics Core at Sylvester Comprehensive Cancer Center to ensure accuracy.

## Results

### Combined Src and EGFR inhibition decreases tumor collagen content and reduces fibrosis in an orthotopic mouse model of PDAC

Collagen is an abundant component of the desmoplastic stroma in PDAC tumors, acting to physically impede intratumoral drug delivery and activate pro-survival pathways which promote chemoresistance (18–20). Previous studies have specifically implicated type IV collagen as a pro-tumorigenic extracellular matrix protein which is highly upregulated in PDAC and functions to enhance tumor cell proliferation and inhibit apoptosis (21,22). To examine the changes in stromal collagen content and fibrosis observed with Src and EGFR inhibition, *in vivo* studies were performed using both BxPC3 and PANC1 orthotopic xenografts. Treatment with indicated compounds was continued in mice for three weeks. Animals were then humanely euthanized and pancreatic tissues were harvested for subsequent histologic analysis. In BxPC3 xenografts, DST or ERL monotherapy failed to significantly reduce either collagen IV or total collagen levels as compared to the vehicle treatment. However, treatment with combined DST/ERL regimen produced a marked decrease in collagen IV levels and trichrome-positive staining area (Fig. 1A). Similarly, single-agent DST or ERL failed to reduce type IV collagen levels or trichrome-positive staining in PANC1 xenografts, but both were significantly decreased by combined DST/ERL treatment (Fig. 1B). We observed a similar reduction in collagen I in PANC1 xenografts (Supplementary Fig. S1). Importantly, the addition of GEM to combined DST/ERL treatment arms did not reverse the anti-fibrotic effects of this therapy, indicating that cytotoxic chemotherapy does not alter the stromal response to combined Src and EGFR inhibition (Fig. 1A and 1B). These results demonstrate that combined Src and EGFR pathway inhibition reduces tumor collagen content and stromal fibrosis *in vivo*.

### Combined Src and EGFR inhibition decreases STAT3 activity and enhances microvessel density in an orthotopic mouse model of PDAC

PDAC tumors are characterized by poor vascular perfusion and profound hypoxia, factors which promote the release of soluble molecules which induce stromal activation, impair drug delivery, and influence tumor progression (23,24). Paradoxically, this hypoxic microenvironment can lead to further perturbations in intratumoral blood vessel formation which worsen tissue perfusion and limit the response to chemotherapeutic agents (25–27). We have previously demonstrated that direct inhibition of the transcription factor STAT3 remodels the TME to increase MVD and thereby improve the delivery of GEM into PDAC tumors, yet the role of combined Src/EGFR inhibition in recapitulating these changes remains unknown (14,16). To confirm target inhibition of STAT3 *in vivo*, BxPC3 xenograft samples were probed for pSTAT3 levels by IHC. In tumors treated with DST or ERL alone,

there was no significant decrease in pSTAT3 when compared to control tissues. However, in combined DST/ERL and DST/ERL/GEM treatment groups, there was a substantial reduction in pSTAT3, confirming our previous findings that concurrent Src and EGFR pathway inhibition functions to reduce STAT3 activation *in vivo* (Fig. 2A). To determine if these changes correlated with a change in the MVD in PDAC tumors, treated samples were probed for CD31 (PECAM-1) levels by IHC. CD31 is an endothelial marker which is associated with vascular normalization and maturity and has been correlated with chemotherapeutic response in previous studies of PDAC (11,28). While we observed no difference between vehicle or single-agent DST/ERL arms, a significant increase in CD31-positive staining was seen in tumors treated with combined DST/ERL which was sustained with the addition of GEM (Fig. 2B). To determine if this increase in MVD correlated with improved intratumoral penetration of GEM, matrix-assisted laser desorption/ionization imaging mass spectrometry (MALDI-IMS) was utilized to examine GEM levels in treated specimens as previously described (14). Levels of GEM were nearly undetectable in tumors treated with ERL or DST monotherapy in combination with GEM. However, combined treatment with DST/ERL was able to markedly increase the detectable levels of GEM within PDAC tumors (Supplementary Fig. S2). Overall, these results suggest that combined Src/EGFR inhibition reduces STAT3 activity and increases the MVD within PDAC tumors, leading to improved delivery of cytotoxic chemotherapy.

**Combined Src and EGFR inhibition reduces tumor growth, decreases stromal fibrosis and STAT3 activation, and increases microvessel density in a spontaneous murine model of PDAC.**

Although orthotopic tumor xenografts are reliable models for studying drug response in PDAC tumors, there are significant limitations which may hinder the use of this model in studying tumor-stromal interactions (29). Therefore, we aimed to determine if the effects of combined Src and EGFR inhibition observed in orthotopic models could be reproduced in an immunocompetent, spontaneous mouse model of PDAC. For these studies, we utilized the PKT mouse model, which develop pancreatic tumors that closely mirror the histologic progression and stromal composition seen in spontaneous human PDAC (15). We have previously demonstrated that this model is characterized by abundant fibrosis, reduced vascular perfusion, and marked resistance to GEM treatment, making it a suitable model to study the effects of combined Src/EGFR inhibition on stromal remodeling in PDAC (14). Treatment with DST, ERL, and GEM either alone or in combination was initiated in PKT mice at 4 weeks of age (n=5–7 per group), at which point mice reproducibly develop locally aggressive tumors. Therapy was continued for 4 weeks and mice were sacrificed and tumors harvested for histologic analysis (Fig. 3A). In PKT tumors, combined DST/ERL or DST/ERL/GEM treatment regimens significantly reduced tumor weight at endpoint (Fig. 3B). Changes in stromal fibrosis were characterized in treated specimens by staining for collagen I, collagen IV, and trichrome blue. Combined DST/ERL treatment was effective in reducing levels of collagen I and IV and overall tumor fibrosis, an effect which was preserved with the addition of GEM (Fig. 3C). Similarly, levels of pSTAT3 were substantially reduced with combined DST/ERL or DST/ERL/GEM treatment in PKT tumor samples (Fig. 4A&B). This was accompanied a compensatory rise in CD31-positive staining in samples treated with DST/ERL or DST/ERL/GEM which was not observed in vehicle or

single-arm treatments (Fig. 4C). Overall, these results validate the findings observed in orthotopic models and demonstrate that combined Src and EGFR inhibition decreases tumor weight, reduces stromal fibrosis, inhibits STAT3 activity, and increases MVD in a spontaneous mouse model of PDAC.

### **Combined Src and EGFR inhibition prevents PDAC tumor progression and improves overall survival in PKT mice**

To determine the effect of combined Src/EGFR inhibition +/- GEM on overall survival, PKT mice were treated beginning at four weeks of age (n=7-9 per group) and continued on therapy until moribund, at which point animals were euthanized (Fig. 5A). Monotherapy with either DST, ERL, or GEM alone was ineffective in improving overall survival. However, combined DST/ERL and DST/ERL/GEM regimens substantially improved survival over vehicle treated mice (median survival of 54 days compared to 99 and 105 days, respectively; p=0.004) (Fig. 5B). To examine the changes in microscopic tumor burden due to targeted therapy, H&E staining was performed on vehicle and treated pancreatic tissue specimens. Microscopic analysis showed that PKT mice treated with vehicle or monotherapy had no reduction in tumor burden. Only combination therapy with DST/ERL/GEM produced a significant reduction in the total tumor relative to normal pancreatic tissue area when compared to PKT mice treated with vehicle or monotherapy alone (Fig. 5C). Importantly, there was no difference in overall weight between treatment arms during therapy (Supplementary Fig. S3). Overall, these findings indicate that combined DST/ERL and DST/ERL/GEM treatment is well-tolerated and improves overall survival in a preclinical mouse model of PDAC.

## **Discussion**

Despite the well-described antitumor effects on primary tumor cells, the role of combined Src/EGFR inhibition on improving the overall survival via altering the stromal composition in PDAC remain unknown. PDAC is characterized by the presence of a dense, desmoplastic stromal reaction which comprises a majority of tumor mass and plays a central role in tumor initiation and progression (30,31). The extracellular matrix in PDAC tumors is comprised of structural proteins such as collagen, laminin, and hyaluronan which act as a physical barrier to effector immune cell infiltration and intratumoral drug delivery (9,32,33). Additionally, the heterogeneous cellular component of the stroma, consisting predominately of cancer-associated fibroblasts (CAFs) and immune cells, also actively engage in crosstalk with PDAC tumor cells through soluble mediators that promote disease progression and modulate therapeutic resistance (34,35). The stroma has been identified as a critical mediator of GEM resistance through numerous mechanisms including upregulation of anti-apoptotic pathways, alterations in the expression of tumor cell nucleoside transporters, or through direct covalent modifications to GEM which block its cytotoxic effects (36-38). Furthermore, PDAC tumors are characterized by profound tissue hypoxia due to poor vascular perfusion and paucity of intratumoral blood vessels, which impairs delivery of chemotherapeutic compounds into tumors (11,39,40). In a sentinel study by Olive et al, depletion of the pancreatic stroma using the Hedgehog inhibitor IPI-926 produced a marked increase in CD31+ staining and an increase in intratumoral GEM delivery, thereby enhancing cellular

apoptosis and improving overall survival in *LSL-Kras<sup>G12D/+</sup>;LSL-Trp53<sup>R172H/+</sup>;Pdx-1-Cre* (KPC) mice (11). Therefore, recent interest has been aimed at identifying agents which target the stromal constituents in PDAC to potentially improve the chemotherapeutic response (41–43).

Despite an abundance of promising preclinical data, pharmacologic inhibition of either the EGFR or Src pathways in combination with cytotoxic chemotherapy has showed limited efficacy in clinical trials of PDAC. In the CONKO-005 trial, there was no observed benefit in disease-free or overall survival with the addition ERL to traditional GEM regimens in the treatment of resectable PDAC (3). Similarly, DST monotherapy has failed to improve the efficacy of GEM in a randomized controlled trial for the treatment of locally advanced PDAC (4). Feedback activation of STAT3 has been identified by our group and others as an essential mediator of resistance to Src and EGFR pathway inhibitors which may account for the lack of clinical efficacy seen with these single-agent regimens (6,8,16,44). Previous studies have demonstrated that monotherapy with either DST or ERL shows only a transient decrease in pSTAT3 levels, with reactivation seen at roughly 24 hours post-treatment. Synchronous inhibition of both the Src and EGFR kinases has been shown to combat these resistance mechanisms through sustained inhibition of the STAT3 pathway, leading to an improvement in GEM efficacy in primary PDAC tumor cells (6,14).

In this study, we demonstrate for the first time that combined Src and EGFR inhibition does not only exert its potent antitumor effects through acting on PDAC tumor cells, but induces dramatic changes in the tumor stroma, resulting in reduced tissue fibrosis and enhanced MVD within the TME. Furthermore, these alterations corresponded to an increase in GEM penetration into xenograft tumors and markedly improved overall survival in PKT mice. Prior investigations by our group and others have specifically highlighted the importance of JAK/STAT signaling in influencing the stromal landscape in PDAC (45). In the present study, we have verified that STAT3 activation is markedly decreased with concurrent EGFR and Src inhibition. Furthermore, the stromal changes observed in this investigation, including an increase in MVD and enhanced intratumoral penetration of GEM, closely mirror those that we and others have observed with STAT3 blockade alone, suggesting that combined Src/EGFR inhibition may mediate these effects on stroma through inhibition of STAT3 (14). However, further mechanistic studies are needed to definitively validate this hypothesis.

Overall, these findings demonstrate a novel mechanism of action of combined Src and EGFR inhibition in promoting stromal remodeling, increasing MVD, and enhancing GEM penetration within PDAC tumors. The therapeutic potential of this regimen is evidenced in a recent phase I trial utilizing DST and ERL in combination with GEM for the treatment of advanced PDAC, which showed encouraging preliminary results (46). The results obtained in the present study provide valuable preclinical insights into the therapeutic benefit of combined Src/EGFR inhibition observed in these patients. As the stromal compartment is essential in mediating tumor progression and effector immune cell infiltration, future mechanistic investigations into the alterations in cytokine signaling and immune populations within the TME produced by DST and ERL treatment should be explored.



## Supplementary Material

Refer to Web version on PubMed Central for supplementary material.

## Acknowledgments:

This work was supported by the American Cancer Society IRG 98-277-13 to N.S. Nagathihalli and NIH R01 CA161976 and NIH T32 CA211034 to N. B. Merchant. A.R. Dosch and B. Willobee are fellows on NIH T32 CA211034. Histopathology Core Service was performed through the Sylvester Comprehensive Cancer Center (SCCC) support grant (N. Merchant and N. Nagathihalli).

## References

1. Hall BR, Cannon A, Atri P, Wichman CS, Smith LM, Ganti AK, et al. Advanced pancreatic cancer: a meta-analysis of clinical trials over thirty years. *Oncotarget* 2018;9:19396–405 [PubMed: 29721211]
2. Matthaios D, Zarogoulidis P, Balgouranidou I, Chatzaki E, Kakolyris S. Molecular pathogenesis of pancreatic cancer and clinical perspectives. *Oncology* 2011;81:259–72 [PubMed: 22116519]
3. Sinn M, Bahra M, Liersch T, Gellert K, Messmann H, Bechstein W, et al. CONKO-005: Adjuvant Chemotherapy With Gemcitabine Plus Erlotinib Versus Gemcitabine Alone in Patients After R0 Resection of Pancreatic Cancer: A Multicenter Randomized Phase III Trial. *J Clin Oncol* 2017;35:3330–7 [PubMed: 28817370]
4. Evans TRJ, Van Cutsem E, Moore MJ, Bazin IS, Rosemurgy A, Bodoky G, et al. Phase 2 placebo-controlled, double-blind trial of dasatinib added to gemcitabine for patients with locally-advanced pancreatic cancer. *Ann Oncol* 2017;28:354–61 [PubMed: 27998964]
5. Lakkakula B, Farran B, Lakkakula S, Peela S, Yarla NS, Bramhachari PV, et al. Small molecule tyrosine kinase inhibitors and pancreatic cancer-Trials and troubles. *Semin Cancer Biol* 2018
6. Jaganathan S, Yue P, Turkson J. Enhanced sensitivity of pancreatic cancer cells to concurrent inhibition of aberrant signal transducer and activator of transcription 3 and epidermal growth factor receptor or Src. *J Pharmacol Exp Ther* 2010;333:373–81 [PubMed: 20100905]
7. Johnson FM, Saigal B, Tran H, Donato NJ. Abrogation of signal transducer and activator of transcription 3 reactivation after Src kinase inhibition results in synergistic antitumor effects. *Clin Cancer Res* 2007;13:4233–44 [PubMed: 17634553]
8. Nagaraj NS, Washington MK, Merchant NB. Combined Blockade of Src Kinase and Epidermal Growth Factor Receptor with Gemcitabine Overcomes STAT3-Mediated Resistance of Inhibition of Pancreatic Tumor Growth. *Clin Cancer Res* 2011;17:483–93 [PubMed: 21266529]
9. Liang C, Shi S, Meng Q, Liang D, Ji S, Zhang B, et al. Complex roles of the stroma in the intrinsic resistance to gemcitabine in pancreatic cancer: where we are and where we are going. *Exp Mol Med* 2017;49:e406 [PubMed: 29611542]
10. Vennin C, Murphy KJ, Morton JP, Cox TR, Pajic M, Timpson P. Reshaping the Tumor Stroma for Treatment of Pancreatic Cancer. *Gastroenterology* 2018;154:820–38 [PubMed: 29287624]
11. Olive KP, Jacobetz MA, Davidson CJ, Gopinathan A, McIntyre D, Honess D, et al. Inhibition of Hedgehog signaling enhances delivery of chemotherapy in a mouse model of pancreatic cancer. *Science* 2009;324:1457–61 [PubMed: 19460966]
12. Rhim AD, Oberstein PE, Thomas DH, Mirek ET, Palermo CF, Sastra SA, et al. Stromal elements act to restrain, rather than support, pancreatic ductal adenocarcinoma. *Cancer Cell* 2014;25:735–47 [PubMed: 24856585]
13. Catenacci DV, Junttila MR, Karrison T, Bahary N, Horiba MN, Nattam SR, et al. Randomized Phase Ib/II Study of Gemcitabine Plus Placebo or Vismodegib, a Hedgehog Pathway Inhibitor, in Patients With Metastatic Pancreatic Cancer. *J Clin Oncol* 2015;33:4284–92 [PubMed: 26527777]
14. Nagathihalli NS, Castellanos JA, Shi C, Beesetty Y, Reyzer ML, Caprioli R, et al. Signal Transducer and Activator of Transcription 3, Mediated Remodeling of the Tumor Microenvironment Results in Enhanced Tumor Drug Delivery in a Mouse Model of Pancreatic Cancer. *Gastroenterology* 2015;149:1932–43 [PubMed: 26255562]

15. Chytil A, Magnuson MA, Wright CV, Moses HL. Conditional inactivation of the TGF-beta type II receptor using Cre:Lox. *Genesis* 2002;32:73–5 [PubMed: 11857781]
16. Nagathihalli NS, Castellanos JA, Lamichhane P, Messaggio F, Shi C, Dai X, et al. Inverse Correlation of STAT3 and MEK Signaling Mediates Resistance to RAS Pathway Inhibition in Pancreatic Cancer. *Cancer Res* 2018;78:6235–46 [PubMed: 30154150]
17. Wu J, Houghton PJ. Interval approach to assessing antitumor activity for tumor xenograft studies. *Pharm Stat* 2010;9:46–54 [PubMed: 19306260]
18. Egeblad M, Rasch MG, Weaver VM. Dynamic interplay between the collagen scaffold and tumor evolution. *Curr Opin Cell Biol* 2010;22:697–706 [PubMed: 20822891]
19. Armstrong T, Packham G, Murphy LB, Bateman AC, Conti JA, Fine DR, et al. Type I collagen promotes the malignant phenotype of pancreatic ductal adenocarcinoma. *Clin Cancer Res* 2004;10:7427–37 [PubMed: 15534120]
20. Sethi T, Rintoul RC, Moore SM, MacKinnon AC, Salter D, Choo C, et al. Extracellular matrix proteins protect small cell lung cancer cells against apoptosis: a mechanism for small cell lung cancer growth and drug resistance in vivo. *Nat Med* 1999;5:662–8 [PubMed: 10371505]
21. Ohlund D, Franklin O, Lundberg E, Lundin C, Sund M. Type IV collagen stimulates pancreatic cancer cell proliferation, migration, and inhibits apoptosis through an autocrine loop. *BMC Cancer* 2013;13:154 [PubMed: 23530721]
22. Ohlund D, Lundin C, Ardnor B, Oman M, Naredi P, Sund M. Type IV collagen is a tumour stroma-derived biomarker for pancreas cancer. *Br J Cancer* 2009;101:91–7 [PubMed: 19491897]
23. Longo V, Brunetti O, Gnani A, Cascinu S, Gasparini G, Lorusso V, et al. Angiogenesis in pancreatic ductal adenocarcinoma: A controversial issue. *Oncotarget* 2016;7:58649–58 [PubMed: 27462915]
24. Provenzano PP, Cuevas C, Chang AE, Goel VK, Von Hoff DD, Hingorani SR. Enzymatic targeting of the stroma ablates physical barriers to treatment of pancreatic ductal adenocarcinoma. *Cancer Cell* 2012;21:418–29 [PubMed: 22439937]
25. Goel S, Duda DG, Xu L, Munn LL, Boucher Y, Fukumura D, et al. Normalization of the vasculature for treatment of cancer and other diseases. *Physiol Rev* 2011;91:1071–121 [PubMed: 21742796]
26. Jain RK. Normalization of tumor vasculature: an emerging concept in antiangiogenic therapy. *Science* 2005;307:58–62 [PubMed: 15637262]
27. Jain RK. Normalizing tumor vasculature with anti-angiogenic therapy: a new paradigm for combination therapy. *Nat Med* 2001;7:987–9 [PubMed: 11533692]
28. Katsuta E, Qi Q, Peng X, Hochwald SN, Yan L, Takabe K. Pancreatic adenocarcinomas with mature blood vessels have better overall survival. *Sci Rep* 2019;9:1310 [PubMed: 30718678]
29. Loukopoulos P, Kanetaka K, Takamura M, Shibata T, Sakamoto M, Hirohashi S. Orthotopic transplantation models of pancreatic adenocarcinoma derived from cell lines and primary tumors and displaying varying metastatic activity. *Pancreas* 2004;29:193–203 [PubMed: 15367885]
30. Apte MV, Park S, Phillips PA, Santucci N, Goldstein D, Kumar RK, et al. Desmoplastic reaction in pancreatic cancer: role of pancreatic stellate cells. *Pancreas* 2004;29:179–87 [PubMed: 15367883]
31. Erkan M, Hausmann S, Michalski CW, Fingerle AA, Dobritz M, Kleeff J, et al. The role of stroma in pancreatic cancer: diagnostic and therapeutic implications. *Nat Rev Gastroenterol Hepatol* 2012;9:454–67 [PubMed: 22710569]
32. Shields MA, Dangi-Garimella S, Redig AJ, Munshi HG. Biochemical role of the collagen-rich tumour microenvironment in pancreatic cancer progression. *Biochem J* 2012;441:541–52 [PubMed: 22187935]
33. Huanwen W, Zhiyong L, Xiaohua S, Xinyu R, Kai W, Tonghua L. Intrinsic chemoresistance to gemcitabine is associated with constitutive and laminin-induced phosphorylation of FAK in pancreatic cancer cell lines. *Mol Cancer* 2009;8:125 [PubMed: 20021699]
34. Hwang RF, Moore T, Arumugam T, Ramachandran V, Amos KD, Rivera A, et al. Cancer-associated stromal fibroblasts promote pancreatic tumor progression. *Cancer Res* 2008;68:918–26 [PubMed: 18245495]
35. Neesse A, Michl P, Frese KK, Feig C, Cook N, Jacobetz MA, et al. Stromal biology and therapy in pancreatic cancer. *Gut* 2011;60:861–8 [PubMed: 20966025]

36. Amit M, Gil Z. Macrophages increase the resistance of pancreatic adenocarcinoma cells to gemcitabine by upregulating cytidine deaminase. *Oncoimmunology* 2013;2:e27231 [PubMed: 24498570]
37. Weizman N, Krelin Y, Shabtay-Orbach A, Amit M, Binenbaum Y, Wong RJ, et al. Macrophages mediate gemcitabine resistance of pancreatic adenocarcinoma by upregulating cytidine deaminase. *Oncogene* 2014;33:3812–9 [PubMed: 23995783]
38. Dangi-Garimella S, Krantz SB, Barron MR, Shields MA, Heiferman MJ, Grippo PJ, et al. Three-dimensional collagen I promotes gemcitabine resistance in pancreatic cancer through MT1-MMP-mediated expression of HMGA2. *Cancer Res* 2011;71:1019–28 [PubMed: 21148071]
39. Sofuni A, Iijima H, Moriyasu F, Nakayama D, Shimizu M, Nakamura K, et al. Differential diagnosis of pancreatic tumors using ultrasound contrast imaging. *J Gastroenterol* 2005;40:518–25 [PubMed: 15942718]
40. Sakamoto H, Kitano M, Suetomi Y, Maekawa K, Takeyama Y, Kudo M. Utility of contrast-enhanced endoscopic ultrasonography for diagnosis of small pancreatic carcinomas. *Ultrasound Med Biol* 2008;34:525–32 [PubMed: 18045768]
41. Bahrami A, Khazaei M, Bagherieh F, Ghayour-Mobarhan M, Maftouh M, Hassanian SM, et al. Targeting stroma in pancreatic cancer: Promises and failures of targeted therapies. *J Cell Physiol* 2017;232:2931–7 [PubMed: 28083912]
42. Elahi-Gedwillo KY, Carlson M, Zettervall J, Provenzano PP. Antifibrotic Therapy Disrupts Stromal Barriers and Modulates the Immune Landscape in Pancreatic Ductal Adenocarcinoma. *Cancer Res* 2019;79:372–86 [PubMed: 30401713]
43. McCarroll JA, Naim S, Sharbeen G, Russia N, Lee J, Kavallaris M, et al. Role of pancreatic stellate cells in chemoresistance in pancreatic cancer. *Front Physiol* 2014;5:141 [PubMed: 24782785]
44. Zhao C, Li H, Lin HJ, Yang S, Lin J, Liang G. Feedback Activation of STAT3 as a Cancer Drug-Resistance Mechanism. *Trends Pharmacol Sci* 2016;37:47–61 [PubMed: 26576830]
45. Wormann SM, Song L, Ai J, Diakopoulos KN, Kurkowski MU, Gorgulu K, et al. Loss of P53 Function Activates JAK2-STAT3 Signaling to Promote Pancreatic Tumor Growth, Stroma Modification, and Gemcitabine Resistance in Mice and Is Associated With Patient Survival. *Gastroenterology* 2016;151:180–93 e12 [PubMed: 27003603]
46. Cardin DB, Goff LW, Chan E, Whisenant JG, Dan Ayers G, Takebe N, et al. Dual Src and EGFR inhibition in combination with gemcitabine in advanced pancreatic cancer: phase I results : A phase I clinical trial. *Invest New Drugs* 2018;36:442–50 [PubMed: 28990119]

**Implications:**

These findings demonstrate that Src/EGFR inhibition targets STAT3, remodels the tumor stroma, and results in enhanced delivery of gemcitabine to improve overall survival in a mouse model of PDAC.

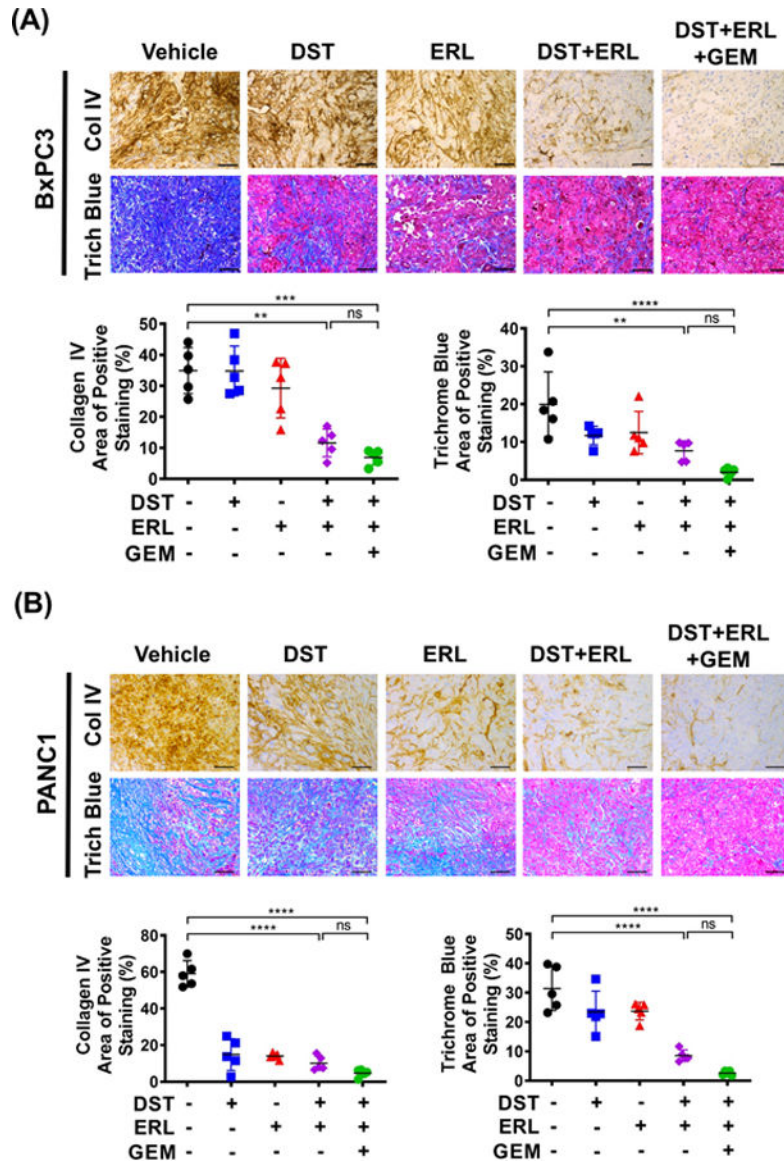


**Figure 1.** Combined Src and EGFR inhibition decreases tumor collagen content and reduces fibrosis in an orthotopic mouse model of PDAC. Orthotopic BxPC3 (A) and PANC1 (B) tumor xenografts were established in nude mice (n=5 per group) and treated with vehicle, dasatinib (DST, 25 mg/kg/daily), erlotinib (ERL, 50 mg/kg/daily), and/or gemcitabine (GEM, 15 mg/kg/every three days) for three weeks prior to sacrifice. IHC was performed for collagen IV and trichrome blue staining in xenograft tumor samples. Representative collagen IV and trichrome blue staining of BxPC3 (A, top panels) and PANC1 (B, top panels) xenograft tissues were shown (scale bar = 50  $\mu$ m). Expression levels of collagen IV and trichrome blue were quantified using Image J from BxPC3 (A, lower panels) and PANC1 (B, lower panels) xenograft tissues and reported as percentage positive staining of total area. ns, nonsignificant; \*\*, p<0.01; \*\*\*, p<0.001; \*\*\*\*, p<0.0001.

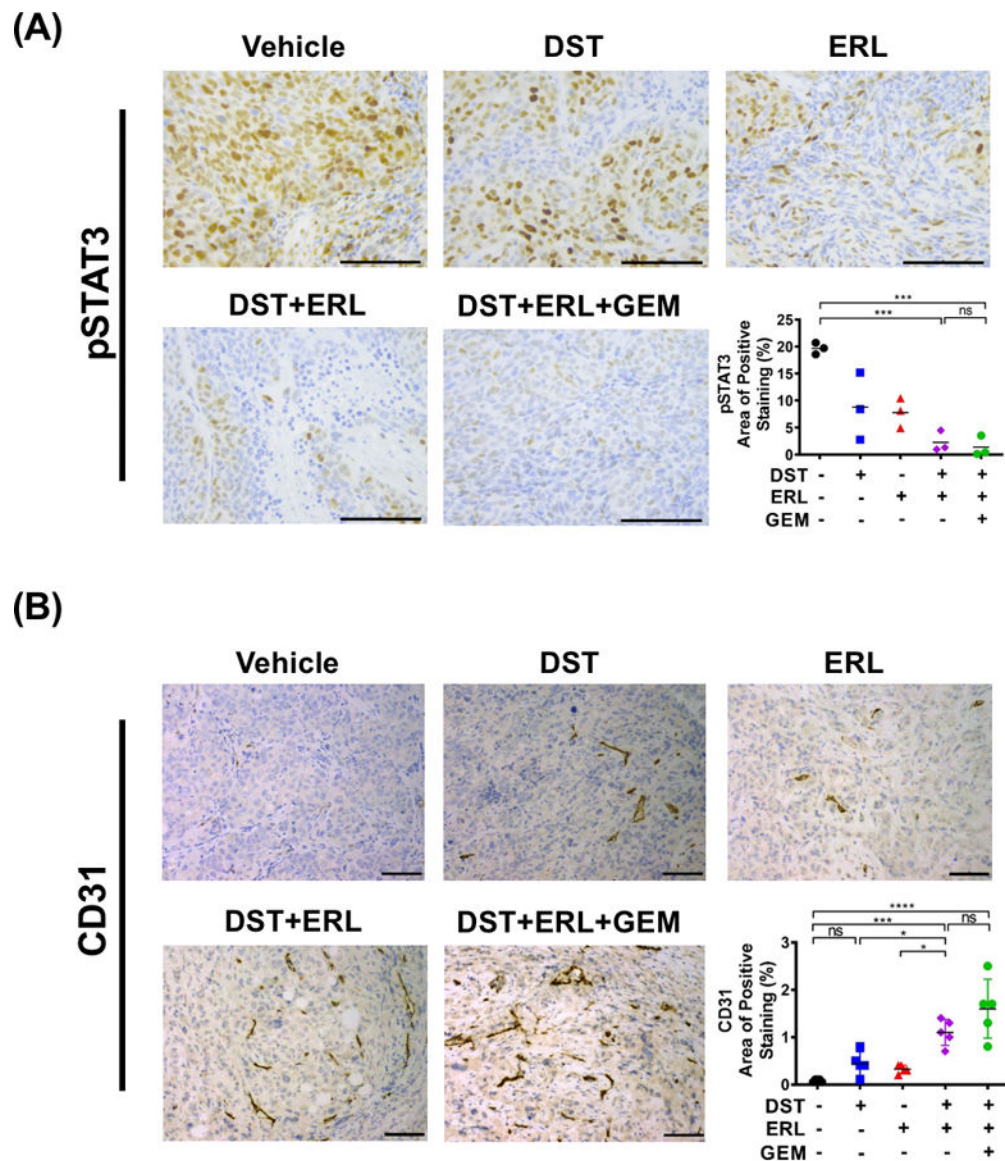


**Figure 2.** Combined Src and EGFR inhibition decreases STAT3 activity and enhances microvessel density in an orthotopic mouse model of PDAC. Histologic analysis was performed for pSTAT3 (A) and CD31 (B) in vehicle, dasatinib (DST, 25 mg/kg/daily), erlotinib (ERL, 50 mg/kg/daily), and/or gemcitabine (GEM, 15 mg/kg/every three days) treated BxPC3 orthotopic tumor xenograft samples (n=3–5 per group, scale bar = 50  $\mu$ m). pSTAT3 (A) and CD31 (B) positive expression levels were analyzed and reported as percentage positive staining of total area. ns, nonsignificant; \*, p<0.05; \*\*, p<0.001; \*\*\*, p<0.0001.

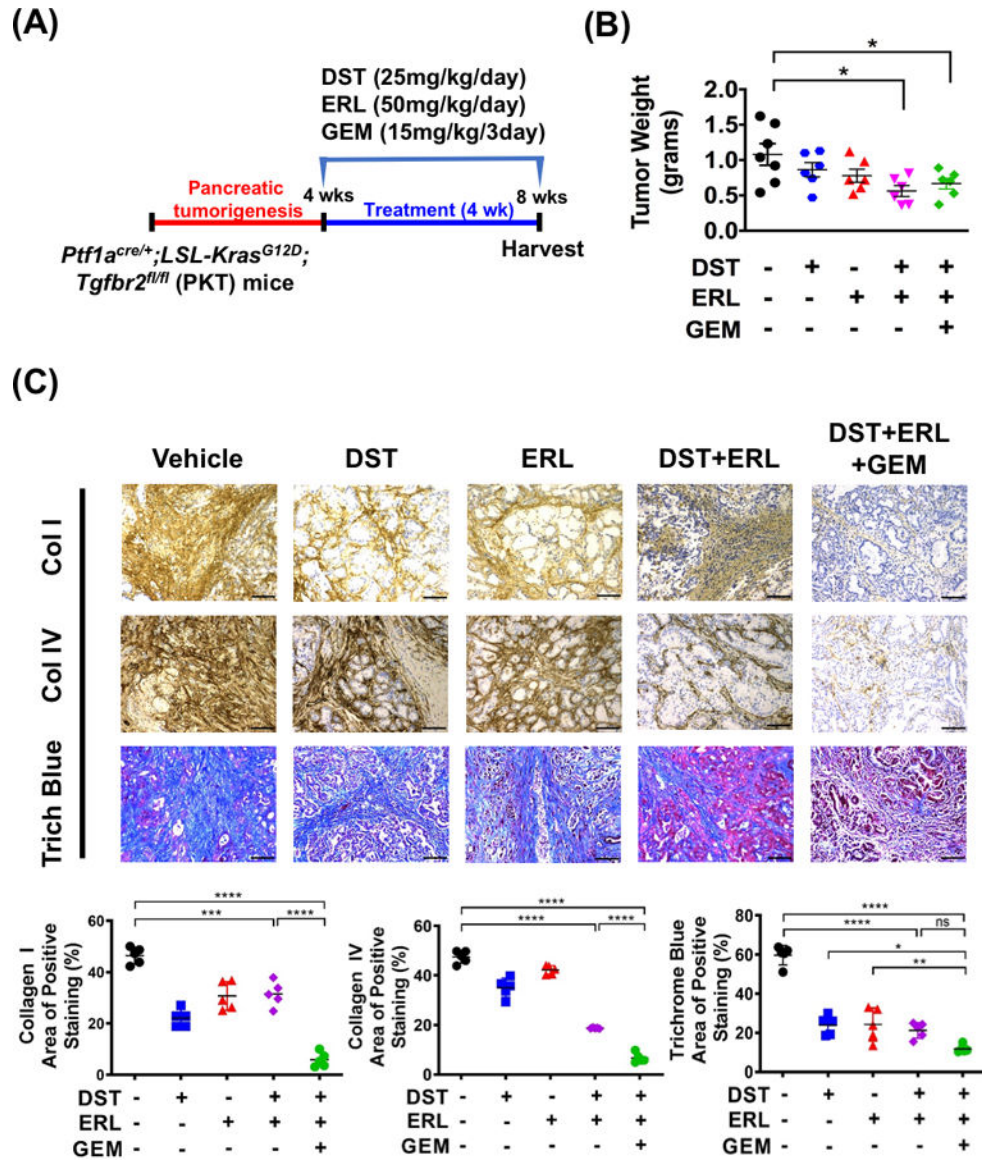


**Figure 3.** Combined Src and EGFR inhibition reduces tumor growth and decreases stromal fibrosis in a spontaneous murine model of PDAC. (A) Treatment of vehicle, dasatinib (DST, 25 mg/kg/daily), erlotinib (ERL, 50 mg/kg/daily), and/or gemcitabine (GEM, 15 mg/kg/every three days) in *Ptf1a<sup>cre/+</sup>;LSL-Kras<sup>G12D</sup>;Tgfb2<sup>fl/fl</sup>* (PKT) mice (n=5–7 per group) was initiated at four weeks of age, when mice reproducibly develop palpable tumors, and continued for four weeks prior to sacrifice. (B) PKT mice tumor weight at sacrifice between vehicle and treated arms was recorded. Representative collagen I, collagen IV and trichrome blue (C, top panels) staining of pancreatic tissues harvested from PKT mice treated with drugs (scale bar = 50  $\mu$ m). Histologic analysis was performed for collagen I, collagen IV, trichrome blue (C, lower panels) in PKT mice. ns, nonsignificant; \*, p<0.05; \*\*, p<0.01; \*\*\*, p<0.001; \*\*\*\*, p<0.0001.

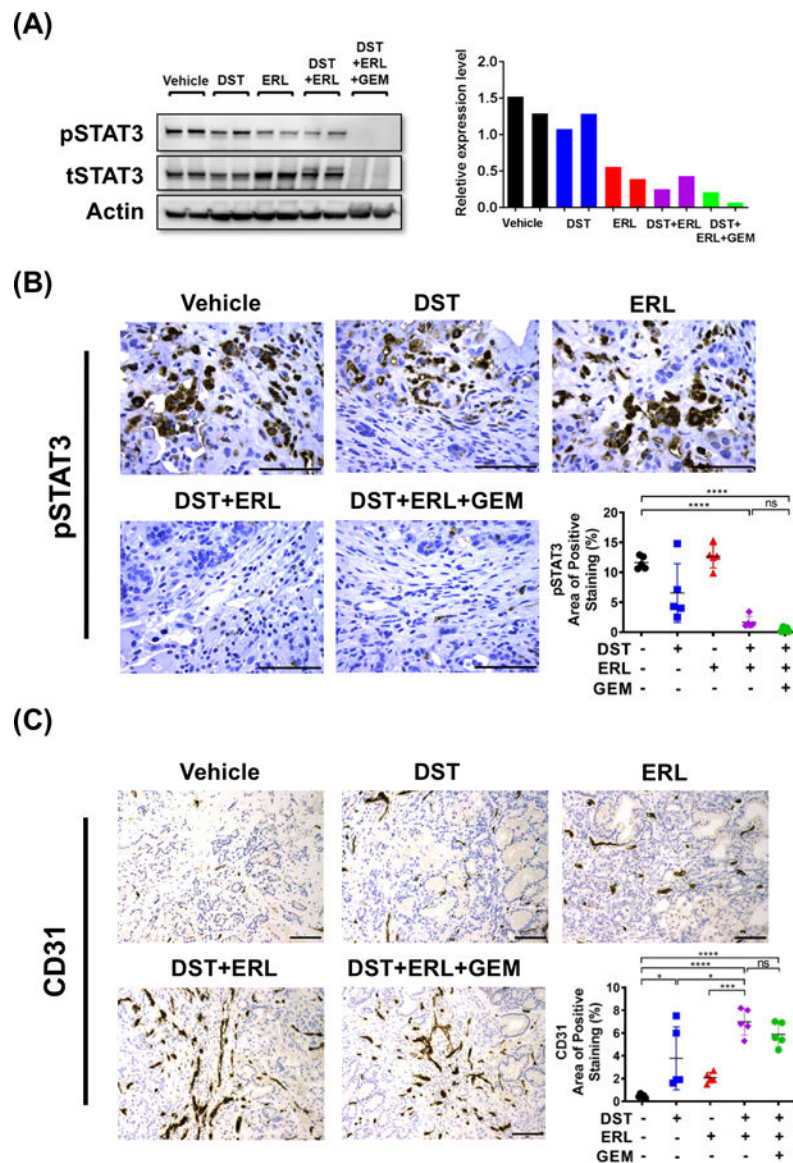


**Figure 4.** Combined Src and EGFR inhibition reduces STAT3 activation and improves tumor microvessel density in PKT mice. (A) Western blot demonstrating levels of pSTAT3 from whole tumor lysate in PKT mice treated with vehicle, dasatinib (DST, 25 mg/kg/daily), erlotinib (ERL, 50 mg/kg/daily), and/or gemcitabine (GEM, 15 mg/kg/every three days) (left panel). Quantification of pSTAT3 levels relative to tSTAT3 levels in treated PKT samples (right panel). Histologic analysis was performed for (B) pSTAT3 and (C) microvessel density was determined by CD31+ staining (scale bar = 50  $\mu$ m). (B) pSTAT3 and (C) CD31 positive expression levels were analyzed and reported as percentage positive staining of total area. ns, nonsignificant; \*,  $p < 0.05$ ; \*\*\*,  $p < 0.001$ ; \*\*\*\*,  $p < 0.0001$ .



